A VEGETATION/LAND USE MAP AND OTHER IMAGE BASED PRODUCTS FOR SANTA FE COUNTY, NEW MEXICO

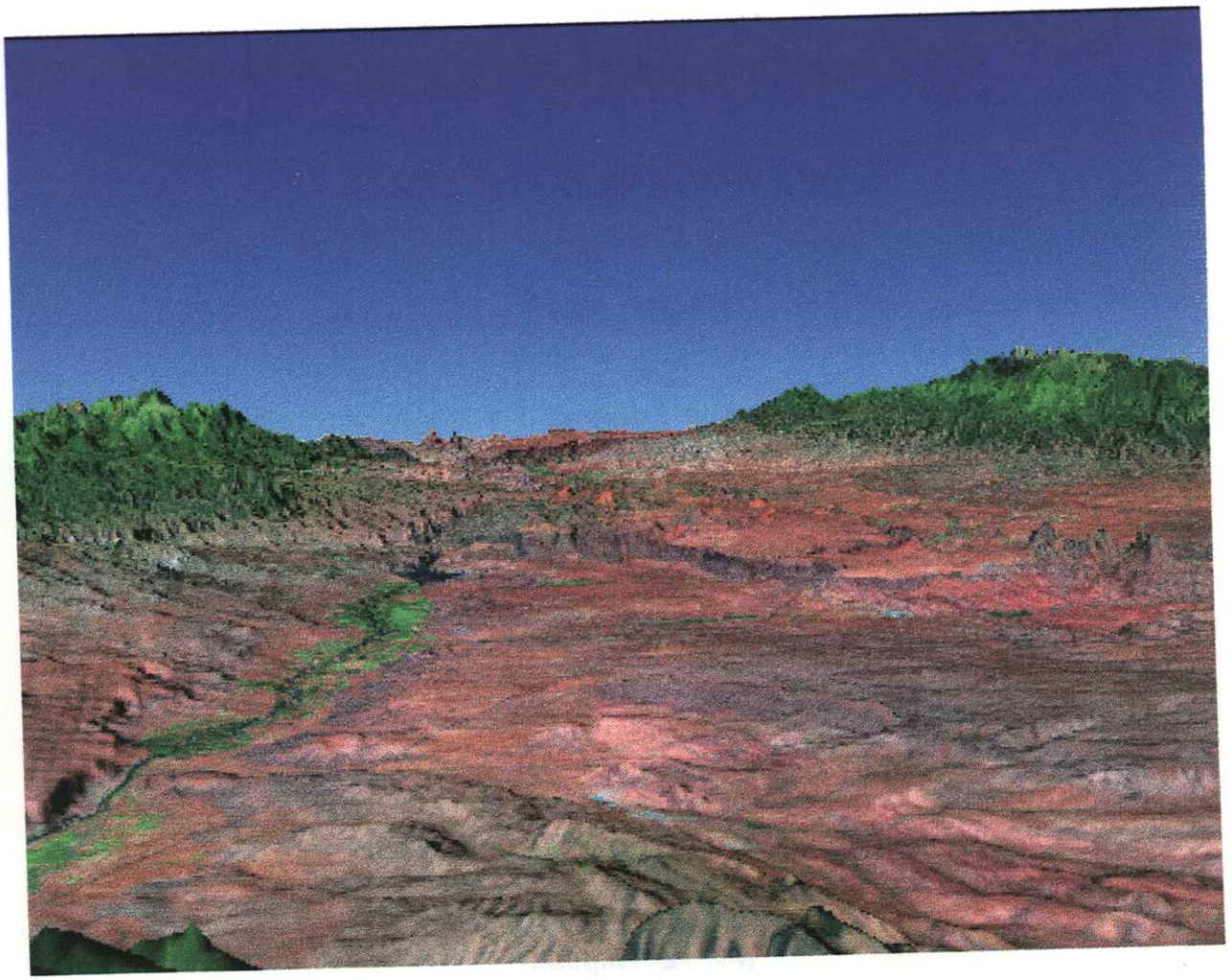

Submitted by:

Earth Data Analysis Center,
University of New Mexico,
Albuquerque, New Mexico

A Vegetation / Land Use Map

And

Other Image Based Products

For

Santa Fe County, New Mexico

Final Report

Submitted to:

Santa Fe County
102 Grant Avenue, P.O. Box 276
Santa Fe, NM 87504-0276

Submitted by

Paul Neville, Teri Bennett, Tom Budge, and Chandra Bales
Earth Data Analysis Center
University of New Mexico
Albuquerque, NM

July, 1998

Table of Contents

Tables

Figures

Introduction

Santa Fe County contracted with the Earth Data Analysis Center (EDAC) at the University of New Mexico in Albuquerque, New Mexico to develop data sets to aid in the hydrologic characterization of the Santa Fe County region as well as for general planning purposes. Specifically, EDAC was to develop maps from Landsat satellite data using both image processing and Geographic Information System (GIS) software. The primary deliverable was a 1:100,000 scale vegetation/land use hard-copy map. The principal use of this map is to serve as a baseline in which to plan from and to assess future changes. In addition, the map in its digital form is a raster-based thematic layer and, as such, is GIS-ready and can be used with other data sets, raster or vector, for hydrologic or planning applications. Other data sets were developed which enhanced various geologic/soil surface features. The development and uses of these data sets are outlined in this document. It was beyond the scope of this project to exactly quantify some of the surface parameters such as soil moisture or to develop an actual surface hydrology model. Further work with these and other more detailed data sets could be used in surface models.

Study Area

Location & Landscape

The study area covers an area 65 miles wide and 102 miles long. It is located in north-central New Mexico between 105° 25" W and 106° 35" W longitude and 34° 54" N and 36° 22" N latitude (Figure 1). This is an area of transition between the Rocky Mountains, Basin and Range, Colorado Plateau, and Great Plains physiographic regions. This region is mainly drained by the Rio Grande. The northwestern portion is drained by the Rio Chama, which enters the Rio Grande near Española. The east central portion is drained by the Pecos River, which enters the Rio Grande much farther to the south in Texas. The major hydrologic basins as well as their sub-watersheds are shown in Figure 2 and listed in Table 1.

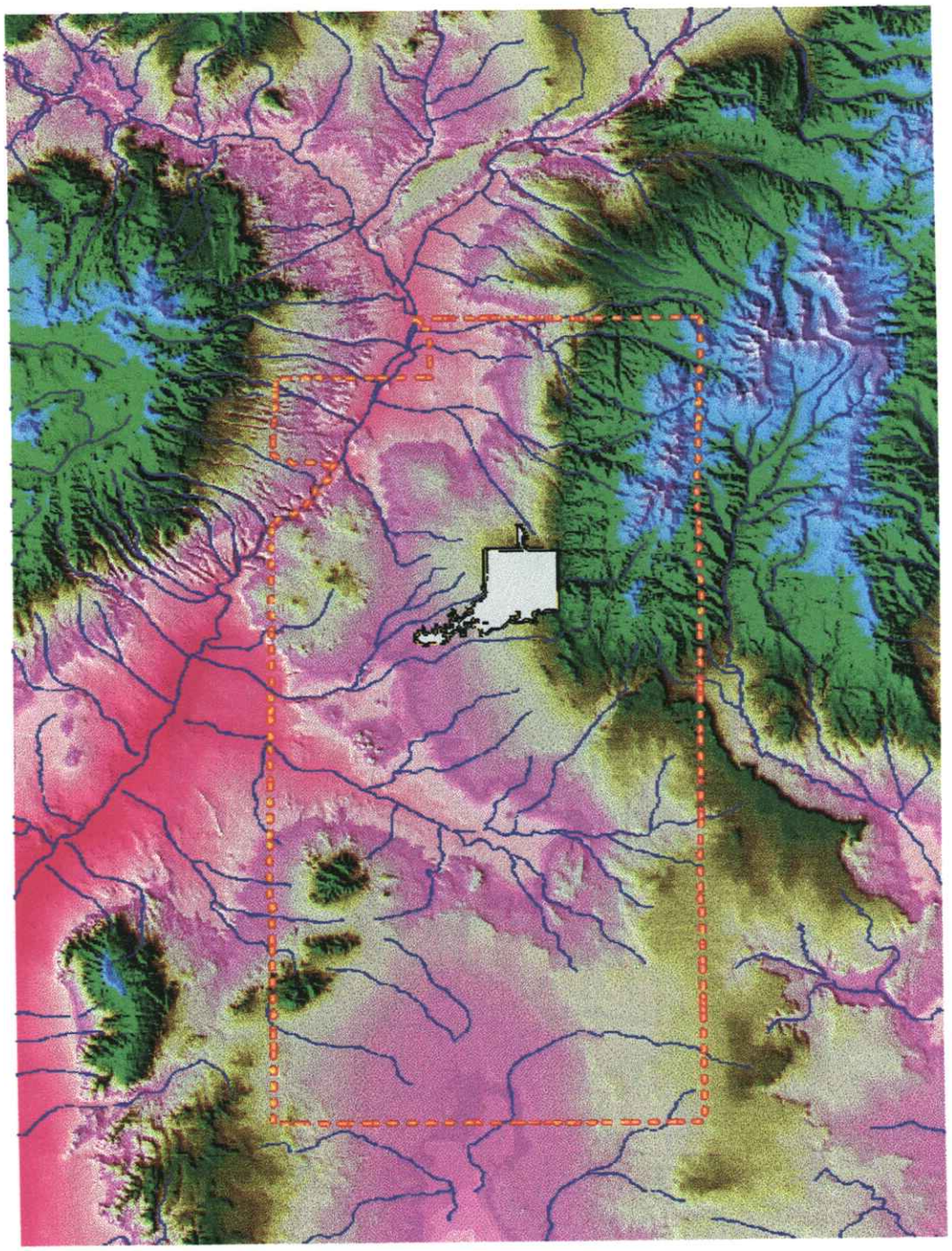

Figure 1. Study area. Shaded relief map with lower elevations represented in reds to the highest elevations in blue. Santa Fe city and county boundaries are delineated and overlain by streams.

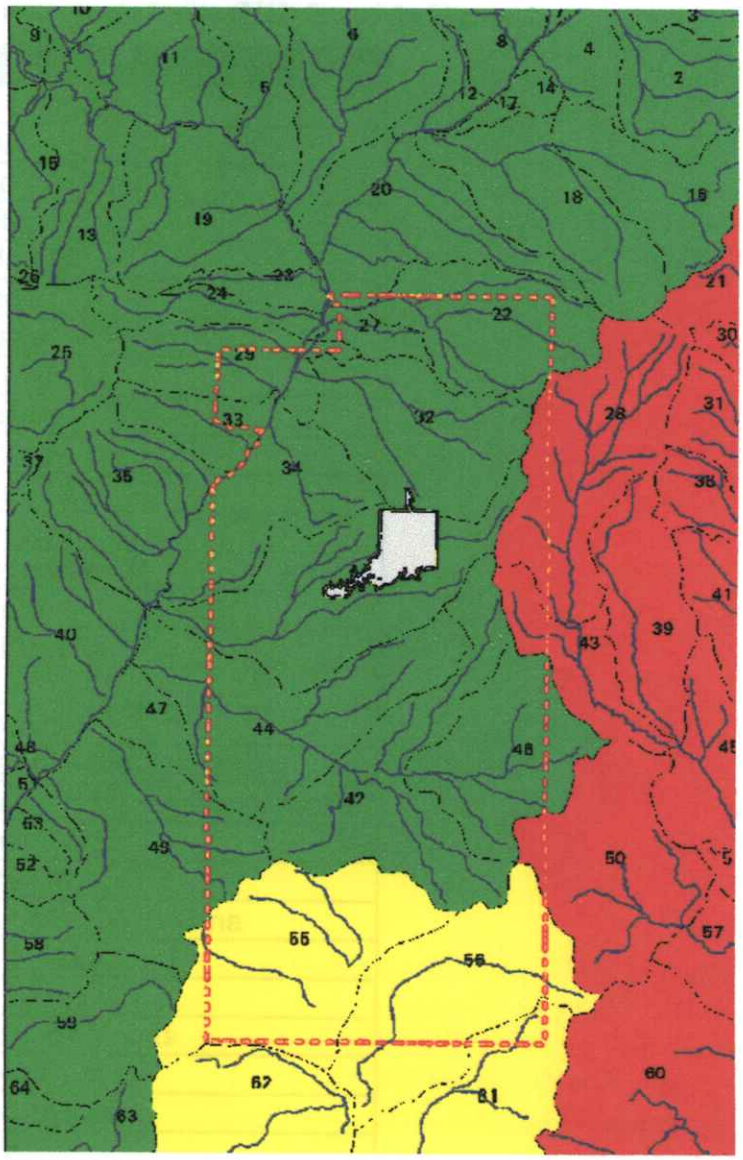

Figure 2. Watershed and sub-watershed boundaries within the study area. Rio Grande watershed in green, Pecos in red, and Estancia in yellow. Numbers refer to sub-watersheds in Table 2.

Table 1. Hydrologic Units (HU) found in Figure 2.

HU#	HU Name
2	Rio Chiquito
3	Taos
4	Little Rio Grande
5	El Rito
6	Gallegos
7	Seco
8	Petaca
9	Rio Cebolla
10	Canjilon
11	Madera
12	Taos TLCP
13	Canones
14	Arroyo Grande
15	Puerco
16	Rio Pueblo
17	Guaje
18	Embudo
19	Espanola-Rio Chama
20	Sebastian Martin-Black Mesa
21	Upper Mora
22	Santa Cruz
23	Espanola-Rio Chama
24	Santa Clara
25	San Diego
26	Rio de las Vacas
27	Arroyo Seco
28	Upper Pecos
29	Guaje
30	Cebolla
31	Sapello
32	Pojoaque
33	White Rock
34	Canada Ancha
35	Bandelier
36	Gallinas
37	San Juan
38	Santa Fe
39	Cow
40	Borrego
41	Tecolote

HU#	HU Name
42	Arroyo de la Jara
43	Rowe
44	Galisteo
45	Carrizito
46	San Cristobal
47	Arroyo de la Vega
48	Zia Pueblo
49	San Pedro
50	Beriero
51	Arroyo Venada
52	Sandia Pueblo
53	Bernalillo
54	Upper Anton Chico
55	Hyer
56	Armijo
57	Canon Blanco
58	Bear
59	Tijeras
60	Palma
61	Big Draw
62	Buffalo Springs
63	Hell's
64	Cedar

The study area is enclosed by basins that range from little relief to being highly dissected terrain. The elevations of these basins range from 5,500 to 8,000 feet and are covered by high desert grassland and shrubland. In the north and central part of the region is the Española Basin which is an asymmetric west-dipping graben dominated by Tertiary fill of the Santa Fe Group. Below the Española Basin is the structurally complex Galisteo Basin that is a series of faulted units ranging from Precambrain crystalline rocks, to Paleozoic, Mesozoic, and Tertiary sediments, to Tertiary and Quaternary volcanics. To the southwest is the east dipping graben known as the Middle Rio Grande or Albuquerque Basin. It is similar to the Española Basin, being mostly filled with Tertiary age Santa Fe Group units. In the southeast is the Estancia Basin that is a sediment-filled trough between the Sandia Mountains and the Pedernal Hills.

These basins are bordered by mountains, the highest of which is Truchas Peak at 13,103 feet. The vegetation ranges from the open conifer woodlands that surround the mountains to the alpine tundra found above the tree-line on the highest peaks. The highest mountains border the east and are known as the Sangre de Cristo Mountains. They have a Precambrian crystalline core which is overlain by Paleozoic and Mesozoic sediments. To the west are the Jemez Mountains. These were created by Tertiary and Quaternary volcanics. To the northwest are the Tusas Mountains that share a similar

geologic history with the Sangre de Cristos. The fault-block Sandia Mountains are found to the southwest.

Climate

The region experiences a dry continental climate with cold winters and hot summers. Temperatures in the basins average in the 30°F. range in the coldest month, January, to the 70°F. range in the hottest month, June (Morris and Haggard, 1985). Temperatures in the mountains can average below 10°F. in January to below 60°F. in June.

Precipitation is seasonally and orographically distributed. Annual precipitation ranges from below 10 inches south of La Bajada Hill to over 30 inches on the highest peaks. Snowfall follows the same spatial distribution ranging from under 12 inches to over 60 inches in the mountains. The driest month is June, which combined with the hottest temperatures, makes it the time of greatest moisture deficit. The summer monsoons begin in July and continue into September bringing most of the precipitation to the area. This moisture combined with the warm temperatures makes this the time of the greatest evapotranspiration. Although snowfall is mainly a mountain phenomenon, the melting of the mountain snowpack provides a substantial recharge for the surrounding aquifers as well as water for the streams and rivers. The water delivered by the riverine systems are in turn used for irrigated agriculture, drinking water, and uptake by riparian vegetation.

Materials & Methods

Satellite Imagery

Landsat Thematic Mapper (TM) satellite imagery was used for mapping the natural vegetation and land cover for the study area. The TM scene used for the project was acquired over the area by the Landsat 5 platform on August 15, 1992 (Figure 3). The image was imported into ERDAS Imagine (Version 8.x) where all raster processing and analysis was done. The TM scene had clouds over half of the Sangre de Cristo Mountains and a few scattered clouds over the Jemez Mountains.

The satellite imagery, with its stable sensor platform, is relatively easy to geometrically correct to known coordinates of a base map. The height of the sensor above the earth (705 km. for Landsat) negates most parallax problems commonly found in aerial photography (parallax is the apparent change in positions of stationary objects affected by the viewing angle – creating greater distortions at greater distances from the center of an aerial photo). Also, satellite data do not have the radiometric problems of air

photos, such as hot spots, dark edges, or different contrasts for each photo due to sun-angle changes during the overflight.

Figure 3. Landsat TM bands 5,4, and 2 shown in red, green, and blue.

The quantitative spectral and spatial aspects of TM imagery add particularly important dimensions to the mapping process. Multi-spectral satellite imagery records the variable reflection of natural radiation of surface materials such as rocks, plants, soils, and water, differently. Variations in plant reflection and absorption due to biochemical composition will register distinct spectral "signatures" (Lillesand and Kiefer 1987). These signatures provide a quantitative measure of reflectance of specific wavelengths which can then be statistically analyzed to develop a vegetation map of spectrally similar plant communities.

Landsat TM has the highest spectral discrimination, with six spectral bands and one thermal band, among commercially available space-based sensors. Each band represents a specific range of light wavelength (Table 2). For vegetation mapping, TM bands 2, 3, 4, 5 and 7 are particularly useful. TM bands 1,3, 5, and 7 are useful for detecting variations in surface geology. Surface geology and soil discrimination are important in developing mapping units in arid and semi-arid areas where the soil response dominates.

TM integrates the spectral characteristics of each band over the Instantaneous Field of View (IFOV) of an area 28.5 m. x 28.5 m.; this is the smallest area resolvable by the sensor and is represented on the computer screen by individual "pixels" (picture elements). Individual occurrences of plants are not resolved by the sensor; therefore, TM is particularly suited for evaluating and quantitatively identifying more generalized vegetation "community" occurrence patterns and their associated surface substrate characteristics.

Table 2. Landsat Thematic Mapper bands and their spectral ranges (derived from Lillesand and Kiefer 1987).

Band	Wavelength (microns)	Spectral Location
1	0.45-0.52	Blue
2	0.52-0.60	Green
3	0.63-0.69	Red
4	0.76-0.90	Near-infrared
5	1.55-1.75	Mid-infrared
6*	10.4-12.5	Thermal Infrared
7	2.08-2.35	Mid-infrared

*TM band 6 has been taken out of the image file used in this project.

Geometric Correction

The TM scene was rectified to a map-based coordinate system using a nearest-neighbor interpolation. This process makes the image planimetric so that area, direction,

and distance measurements can be performed. The image-to-map rectification process involves selecting a point on the map with its coordinate and the same point on the image with its x and y coordinate. The root mean square error (RMS_{error}) is computed to determine how well the map and image coordinates fit in a least-squares regression equation. The RMS_{error} for this image was 0.98 pixel error (or approximately 90 feet). This image was originally projected into UTM, Zone 13, using the 1984 World Geodetic System Datum and the Geodetic Reference Spheroid 1980. The final products were re-projected into the State Plane projection, Central New Mexico Zone (Zone 4751).

Radiometric Correction

A radiometric correction was performed on all TM bands to account for the systematic signal distortion of the sensor. One major source of distortion that occurs is the sensor offset, the residual "black noise" that is recorded by the sensor when there is no input signal (Lillesand and Kiefer, 1987). The other major distortion is from the channel gain, which is the slope transfer relation between the signal received and the sensor's response. Differential offsets and gains between bands will cause problems when comparing their responses to a certain feature, so it is necessary to calibrate all the bands to each other. Gain and offset coefficients for each band are provided for by EOSAT for Landsat TM5 in the original header. The effect of these deviations on the original data are modeled using Equation 1:

$$L = (DN * Gain) + Offset \quad \text{(Eq. 1)}$$

where **L** is the radiometrically corrected signal and **DN** is the input digital number value. The gains and offsets found in Table 3 were used to transform the image DN values.

Table 3. Gains and offsets used to radiometrically calibrate the image data.

	TM1	TM2	TM3	TM4	TM5	TM7
OFFSET	-0.15	-0.280487	-0.119403	-0.15	-0.014999	-0.014999
GAIN	0.0602436	0.1175036	0.0805971	0.0815399	0.0108074	0.0056984

Image Enhancements

Normalized Difference Vegetation Index

The Normalized Difference Vegetation Index (NDVI) was created using Equation 2.

$$NDVI = (TM4 - TM3) / (TM4 + TM3) \quad \text{(Eq. 2)}$$

The NDVI enhances vigorous vegetation over other major surface features. This enhancement helps to emphasize vegetation response patterns in the classification over soil responses and was used as such. The NDVI also allows quick assessment of class signatures: for example, riparian areas should have a higher NDVI response than senescent grasslands. The NDVI has also been found to directly correlate to actual evapotranspiration (AET) and a number of methods have been used to calibrate the NDVI numbers to AET (Culler, *et al.*, 1976, Bastiaanssen, *et al.*, 1996, Choudhury, *et al.*, 1994, and Carlson *et al.*, 1995). Calculating AET was beyond the scope of this project.

Band Ratios

A similar strategy was used to enhance geologic/soil features. Band ratios were created (Figure 5) to emphasize iron-staining (Equation 3), sands and carbonates (Equation 4), and clays (Equation 5).

$$FEOI = TM3/TM1 \quad \text{(Eq. 3)}$$

$$RI = TM5/TM4 \quad \text{(Eq. 4)}$$

$$CI = TM5/TM7 \quad \text{(Eq. 5)}$$

These have been used in numerous geologic studies and are generally reliable indicators (Sabins, 1987). An advantage of band ratioing is that it will tend to suppress differential illumination due to topography. A major problem with the CI ratio is that it emphasizes a similar absorption feature found for well-watered vegetation. A way around this is to display the CI with the NDVI; where both images are bright is well-watered vegetation such as agricultural fields or riparian areas, although clays are entirely likely in those locations. The FEOI will also enhance water, shadows and clouds.

Feature Oriented Principal Components Analysis

Feature Oriented Principal Component Analysis (FOPCA) uses principal component analysis on specific bands in order to enhance specific surface features. In this case the FOPCA technique (Figure 6) was used to enhance similar geologic/soil features enhanced by the band ratios. The equations derived from the FOPCA created a sand/carbonate image (Equation 6), an iron-staining image (Equation 7), and a clay image (Equation 8).

$$FOPCA1 = (0.3*TM1)+(0.21*TM4)+(0.784*TM5)+(0.495*TM7) \quad \text{(Eq. 6)}$$

$$FOPCA2 = (-0.598*TM1)+(0.8*TM3)-(0.12*TM5) \quad \text{(Eq. 7)}$$

$$FOPCA3 = (0.169*TM1)-(0.197*TM4)+(0.496*TM5)-(0.829*TM7) \quad \text{(Eq. 8)}$$

This technique tends to more precisely model these features for a specific area and do not have the same problems with unintentionally enhancing other features such as the band ratios do. They do not suppress topography and are not as widely used as the band ratio technique and therefore both were included in this study. This technique was originally used to enhance mineral alteration patterns in imagery from Brazil, where, despite pervasive vegetation cover, it was able to detect the underlying soil differences (Crosta and Moore, 1989).

Soil Indices

Two images were created to characterize different soil moisture and organic content (Figure 7). The soil moisture index (SMI) was created using Equation 9:

$$SMI = (-11.38*TM1)+(12.17*TM2)-(4.92*TM3)+(1.04*TM4)+(1.67*TM7) \quad \text{(Eq. 9)}$$

The soil organic content index (SOI) was created using Equation 10:

$$SOI = (-0.24*TM1)+(0.33*TM4) \quad \text{(Eq. 10)}$$

These indices are based on work done on soils in Alabama (Coleman and Montgomery, 1987) and should be treated with some discretion. They found the least reliable index was the SOI. Nonetheless, the indices' responses in the study area seemed to correlate with what is expected on the ground and therefore may provide at least a good approximation of surface conditions. The SOI does tend to be influenced in areas of low vegetation cover by clays or humic lithologies. Further research could help determine equations which better fit this region's soil and climate. In addition, field data would be needed to calibrate the image values to actual values.

Ground Survey Data

The mapping process used here is dependent on ground data to develop the map. A set of 173 vegetation/land use plots were collected from the study area from October, 1997 to May, 1998. These points were located using image maps and from coordinates collected by GPS. Points were collected in all major regions covered by the project. Sampling design was based on the image as it was directed towards large polygons of uniform spectral characteristics distributed throughout the study area. In all cases it was attempted to collect points in the center of stands of more or less uniform vegetation or

land use. Each point was recorded on a sheet in the field with its location and a brief description of the class type and other information that would be helpful later to model it on the image.

Image Classification

Supervised Strategy and Seeding

The image classification procedure synthesizes satellite image data with field plot data and ancillary data derived principally from geographic information system (GIS) coverages. A supervised classification strategy was adopted to create the map. This strategy develops spectral classes based on precise ground locations with known characteristics such as vegetation composition, rock type, and landscape context.

In a supervised classification strategy, the field data are applied to the image data through an interactive process called "seeding." In the seeding process, a pixel at the field plot location was selected in the imagery and its spectral characteristics were used to gather other similar contiguous pixels to create a statistical model or "seed" of the field plot. The seeding algorithm searches around that point within user-defined parameters which contain a seed within: 1) a certain distance, 2) a certain area, and 3) a certain spectral distance defined as in Equation 11:

$$SD = \sqrt{\Sigma(\mu - X)^2} \quad \text{(Eq. 11)}$$

where **SD** is the spectral distance between a new pixel and the mean of the current seed group pixels across all bands, μ is the mean of the seed pixel group for each image band, and **X** is the spectral value of the new pixel for each band (ERDAS, 1997).

In an iterative process, the best seed models were constructed by adjusting the parameters and comparing the resulting pixel distributions against the terrain models and the original imagery. A seed was developed for each field plot using the plot GPS location and associated field information. The seed's maximum area was initially defined by the size of the vegetation community occurrence as determined in the field. The actual seed was then defined by increasing the spectral distance iteratively until the spectral signature collected within the seed generated a covariance matrix which could be inverted, a requirement for the maximum likelihood decision rule used later in the actual classification.

The seed shape and location was checked against field notes and maps, and by direct interpretation of the seed in the image on the screen in conjunction with the terrain models. Each seed is saved in a signature file with its field plot number, mean values for

each image band, variance, number of pixels that were used to create the seed, and minimum and maximum values.

Supervised Classification

A supervised classification was performed using the statistics gathered in the seeding process, and is based on a maximum likelihood decision rule. The maximum likelihood decision rule also contains a Bayesian classifier which uses probabilities to weight the classification towards particular classes. In this study the probabilities were unknown, so the maximum likelihood equation for each of the classes is given in Equation 12 as:

$$D = [0.5\ln(cov_c)]-[0.5(X-M_c)^T * (cov_c^{-1})*(X-M_c)] \text{ (Eq. 12)}$$

where **D** is the weighted distance, $\mathbf{cov_c}$ is the covariance matrix for a particular class, X is the measurement vector of the pixel, $\mathbf{M_c}$ is the mean vector of the class and ^{T} is the matrix transpose function (ERDAS,1997). Each pixel is then assigned to the class with the lowest weighted distance. This technique assumes the statistical signatures have a normal distribution.

This decision rule is considered the most accurate, because it not only uses a spectral distance (as the minimum distance decision rule), but it also takes into account the variance of each of the signatures. The variance is important when comparing a pixel to a signature representing, for example, a desert scrub class which is fairly heterogeneous, to a water class, which is more homogeneous.

To locate problems, informal accuracy checking was used based on independent field data, air photos, personal knowledge of a site and other ancillary data. If a distribution problem with a seed was detected, the seed was rechecked to insure it was properly modeling the vegetation type and landscape.

Map Unit Development

A preliminary map was created with as many map classes as seeds used to develop it. The seed map classes were then aggregated into a limited number of Mapping Units (MU's) for the final map. These are based on floristic composition, landscape position, spatial contiguity and spectral similarity, e.g. floristically similar seed classes which had similar landscape positions and were spatially near each other, were grouped into a mapping unit. This was an iterative process based on informal accuracy checking that was continued until all seed classes were grouped into the most consistent and accurate mapping units. The community types listed in Dick-Peddie (1993) were used as a guideline for the creation of the map units for this map.

Results

Map Units

Thirty seven map units were defined (Table 4) for this map (Figure 4). There are 2 classes that are tundra (17,400 acres), 5 classes that are forest (969,132 acres), 2 classes that are scrub (101,434 acres), 6 classes that are woodland (1,696,465 acres), 2 classes that are shrubland (194,336 acres), 8 classes that are grassland (957,539 acres), 4 classes that are riparian (38,509 acres), and 5 classes that are directly related to human disturbance (96,024 acres). Three of the grassland classes (Classes 22, 23, and 25) representing 308,906 acres may also be the result of human impact through grazing as well as some of the juniper savanna class (Class 14) and sagebrush class (Class 16). Two classes (Class 17 and 29) can represent strongly saline soils (13,145 acres). Detailed descriptions of each map unit are provided in Appendix A.

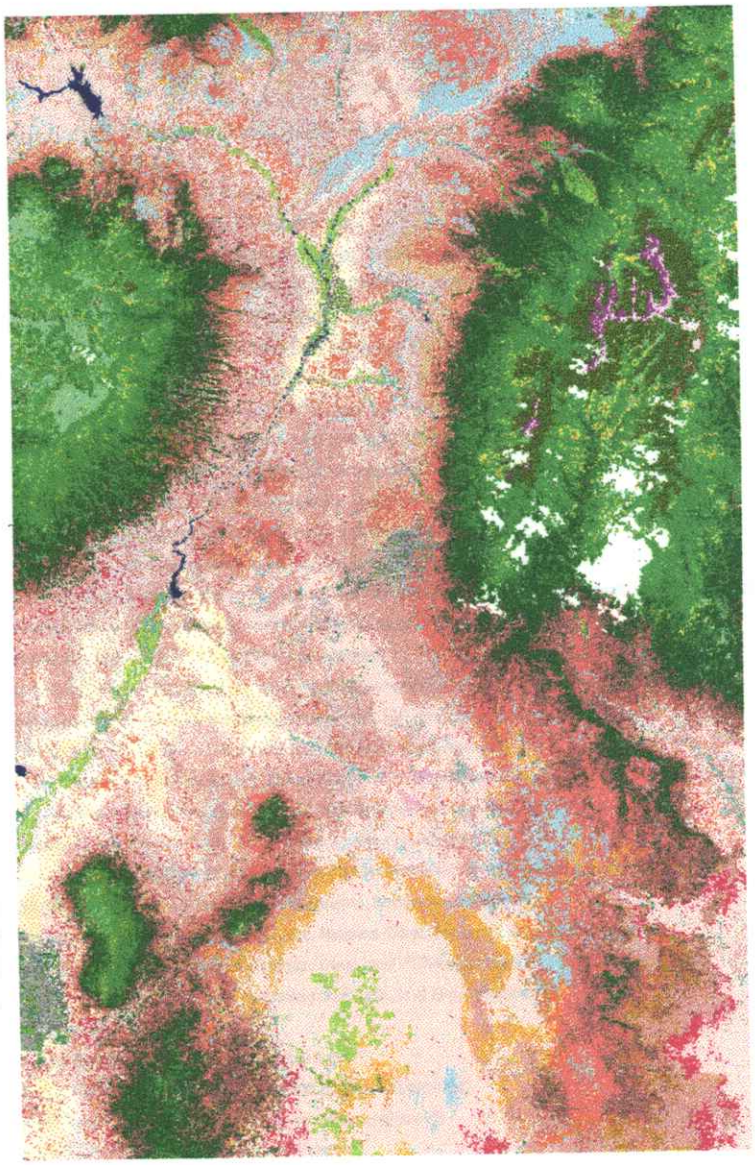

Figure 4. Vegetation classification for the study area. Color key is found on the following page.


Legend
Description
Alpine Tundra Vegetation (Sedges, Avens, and Willow species)
Alpine Tundra Rock Field
Subalpine Broadleaf Forest (Aspen)
Subalpine Conifer Forest (Englemann Spruce)
Subalpine Conifer Forest (Englemann Spruce, Subalpine fir, and Aspen)
Upper Montane Conifer Forest (Douglas-fir, Whiter Fir, and Blue Spruce)
Lower Montane Conifer Forest (Ponderosa Pine)
Montane Deciduous Scrub (Gambel Oak, Mountain Mahogany, and New Mexico Locust)
Evergreen Interior Chaparral (Scrub Oak, Wavyleaf Oak, and Mountain Mahogany)
Closed Conifer Woodland (Pinyon with Juniper and Oak Species)
Closed Conifer Woodland (Pinyon and One-Seed Juniper with Grama grasses)
Closed Conifer Woodland (Pinyon and One-Seed Juniper with sparse ground cover)
Open Conifer Woodland (One Seed Juniper with Oak species)
Open Conifer Woodland (One-Seed Juniper with Grama grasses)
Open Conifer Woodland (One-Seed Juniper with sparse ground cover)
Microphyllous Desert Shrubland (Bigleaf and Sand Sagebrush with Rabbitbrush and Fourwing Saltbush
Microphyllous Desert Shrubland (Fourwing Saltbush with Greasewood)
Subalpine/Montane Grassland (Fescue species)
Mid-Grass Prairie (Needlegrass mixed with other grass species)
Mid-Grass Prairie (Side-Oats Grama mixed with Beargrass and other grass species)
Short-Grass Prairie (Blue Grama mixed with other grass species)
Short Grass Prairie (Blue Grama mixed with Cholla, Sagebrush, Juniper and other grass species)
Short-Grass Prairie (Blue Grama mixed with Snakeweed and other grass species)
Desert Grassland (Black Grama mixed with other grass species)
Desert Grassland (Black Grama mixed with Snakeweed and other grass species)
Montane Riparian/Wetlands (Willow species, Sedges and Rushes)
Riverine Bosque (Cottonwood species, Russian Olive, Tamarisk, and Willow species)
Riverine Woodland (Tamarisk, Russian Olive, and Willow species)
Arroyo Shrubland (Tamarisk, Fourwing Saltbush, and Greasewood)
Irrigated Agriculture
Parks, Golf Courses, and Irrigated Pastures
Mesic Rural/Residential (Mixed tree and irrigated grasses)
Xeric Residential/Urban (Barren or sparsely vegetated)
Manmade Barren (Roads, dams, and etc...)
Rock Outcrop/Talus/Barren or Sparsely Vegetated
Surface Water
Clouds and Shadows

Table 4. Santa Fe region vegetation map units.

No.	Vegetation or Land Use Class	Acres
	Alpine Tundra	
1	Vegetation (Sedges, Avens, and Willow species)	7,242
2	Rock Field	10,158
	Forest	
3	Subalpine Broadleaf Forest (Aspen)	48,757
4	Subalpine Conifer Forest (Englemann Spruce)	100,120
5	Subalpine Conifer Forest (Englemann Spruce, Subalpine Fir, and Aspen)	168,160
6	Upper Montane Conifer Forest (Douglas-fir, White Fir, and Blue Spruce)	266,897
7	Lower Montane Conifer Forest (Ponderosa Pine)	385,198
	Scrub	
8	Montane Deciduous Scrub (Gambel Oak, Mountain Mahogany, and New Mexico Locust)	58,186
9	Evergreen Interior Chaparral (Scrub Oak, Wavyleaf Oak, and Mountain Mahogany)	43,298
	Woodland	
10	Closed Conifer Woodland (Pinyon with Juniper and Oak species)	368,691
11	Closed Conifer Woodland (Pinyon and One-Seed Juniper with Grama grasses)	335,982
12	Closed Conifer Woodland (Pinyon and One-Seed Juniper with sparse ground cover)	83,326
13	Open Conifer Woodland (One-Seed Juniper with Oak species)	24,003
14	Open Conifer Woodland (One-Seed Juniper with Grama grasses)	634,683
15	Open Conifer Woodland (One-Seed Juniper with sparse ground cover)	249,780
Shrubland		
16	Microphyllous Desert Shrubland (Bigleaf and Sand Sagebrush with Rabbitbrush and Fourwing Saltbush)	184,642
17	Microphyllous Desert Shrubland (Fourwing Saltbush with Greasewood)	9,694
	Grassland	
18	Subalpine/Montane Grassland (Fescue species)	64,202
19	Mid-Grass Prairie (Needlegrass species with other grass species)	16,830
20	Mid-Grass Prairie (Side-Oats Grama mixed with Beargrass and other grass species)	34,791
21	Short-Grass Prairie (Blue Grama mixed with other grass species)	497,057
22	Short-Grass Prairie (Blue Grama mixed with Cholla, Sagebrush, Juniper and other grass species)	70,331
23	Short-Grass Prairie (Blue Grama mixed with Snakeweed and other grass species)	111,326
24	Desert Grassland (Black Grama mixed with other grass species)	35,753
25	Desert Grassland (Black Grama mixed with Snakeweed and other grass species)	127,249
	Riparian	
26	Montane Riparian/Wetlands (Willow species, Sedges and Rushes)	5,898

No.	Vegetation or Land Use Class	Acres
27	Riverine Bosque (Cottonwood species, Russian Olive, Tamarisk, and Willow species)	25,674
28	Riverine Woodland (Tamarisk, Russian Olive, and Willow species)	3,486
29	Arroyo Shrubland (Tamarisk, Fourwing Saltbush, and Greasewood)	3,451
	Human Disturbance	
30	Irrigated Agriculture	38,151
31	Parks, Golf Courses, and Irrigated Pastures	4,835
32	Mesic Rural/Residential (Mixed trees and irrigated grasses)	14,542
33	Xeric Residential/Urban (Barren or sparsely vegetated)	18,815
34	Manmade Barren (Roads, dams, and etc...)	19,681
	Other	
35	Rock Outcrop/Talus/Barren or Sparsely Vegetated	60,808
36	Surface Water	6,457
37	Clouds and Shadows	53,483

The Final Map

Although not formally validated, the map was inspected during a two day field check and is believed to accurately reflect the vegetation cover and land use at its intended scale of 1:100,000 (1°x30" USGS quadrangle size). Due to the nature of spectral signatures, the minimum size that can be adequately classified is a class represented by a 3x3 pixel grid (approximately 1.5 acres). Due to the spatial constraints of the satellite data, linear features such as riparian areas are harder to classify. No attempt was made to classify wetlands and they, in general, have been mapped into riparian classes. The heterogeneous nature of human disturbance, spectral band-width, and spatial limitations makes it near impossible to find unique signatures; therefore, natural classes were used to do the original classification over areas of human disturbance. These classes were then recoded using GIS layers or photo-interpretation to a human disturbance class (i.e. a montane grassland became a park class; a sparse class became an urban xeric class). Lastly, although it was classified based on 1997-1998 field notes, the original data is from 1992 and there may be changes from what is there now compared to what it was in the past.

The map units were designed to both accurately reflect the vegetation cover or land use of the area and also to be optimally useful for natural resources management at that scale. Use of the map at finer scales is not recommended without review (additional ground truthing). The map has been made available both in hard copy form and in a digital format suitable for integration into the installation GIS.

Discussion

TM Image Display

As was noted in the Satellite Imagery section and in Table 1, there are a number of bands available with Landsat TM imagery. There are several band combinations that are used as standard displays. A display of TM 3, TM 2, and TM 1 in red, green, and blue (RGB) creates a pseudo natural color display as the red reflecting surfaces are displayed with red, the green reflecting surfaces are displayed in green, and blue reflecting surfaces are displayed in blue. This tends to be the least descriptive False Color Composite (FCC). Water will tend to be black, blue or red depending on sediment load or depth. Vegetation will be a dark green. Iron-stained soils will be yellow to red depending on if it is limonitic or hematitic staining. Most everything else will be a variation of gray to brown.

Another FCC is to display TM 4, TM 3, and TM 2 in RGB. This display enhances vegetation health as shades of red. Iron-staining will be yellow. Water will be black, blue, or green. All other features will be gray to blue-green.

Displays that enhance geologic features are TM 5, TM 4, and TM 2 and TM 7, TM 4, and TM 2 (**NOTE: TM band 6 has been taken out of the image and therefore read TM 7, TM 4, and TM 2 as bands 6, 4, and 2**). The TM 5, TM 4, and TM 2 FCC looks more like a natural display (Figure 3); it enhances lithologic discrimination better than the TM 3, TM 2, and TM 1 FCC. The TM 7, TM 4, and TM 2 FCC looks similar to the TM 5, TM 4, and TM 2 FCC, but gypsum and some clays have little response in TM 7 and therefore they will appear blue-green.

Geologic Enhancements

As mentioned previously, several enhancements were created to give a better idea as to what the lithologic composition was on the ground. Each of these enhancements can be viewed individually as an intensity image denoting where the highest concentrations of a certain surface feature are located or, for better interpretation, combined with the other enhancements in a FCC.

The band ratios are ordered such that the CI is band 1, the RI is in band 2, and the FEOI is in band 3. Displaying this image in a 3, 2, and 1 FCC in RGB shows iron-stained silts and sands reddish orange, iron-stained clays are purple, clays are blue, and sands and carbonates are yellow to green (Figure 5). There are also non-geologic features that are enhanced. Vegetation is blue, and clouds, shadows, and surface water are red to purple.

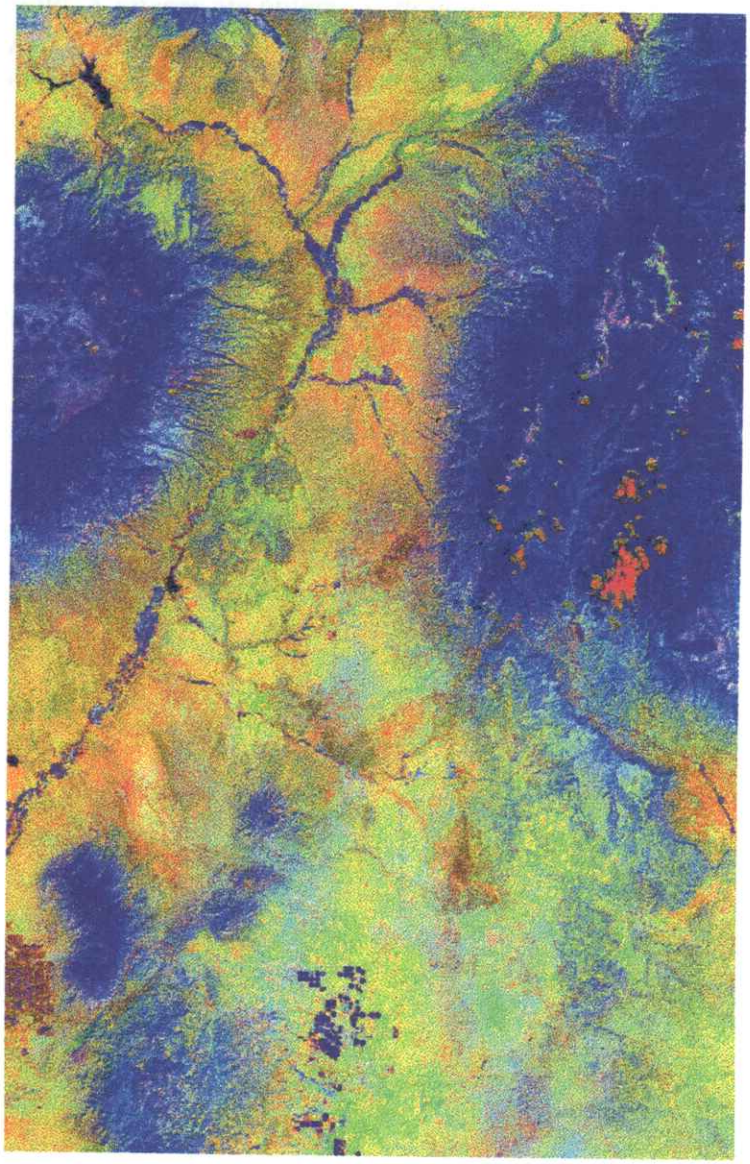

Figure 5. Band ratio image. FEOI in red, RI in green, and CI in blue.

The FOPCA images are ordered with FOPCA1, FOPCA2, and FOPCA3 in bands 1, 2, and 3. A 2, 1, and 3 FCC displays the geology in the same way as the band ratio FCC mentioned above (Figure 6), but more subtle details tend to be enhanced. In addition, gypsum appears bright blue-green and vegetation is dark.

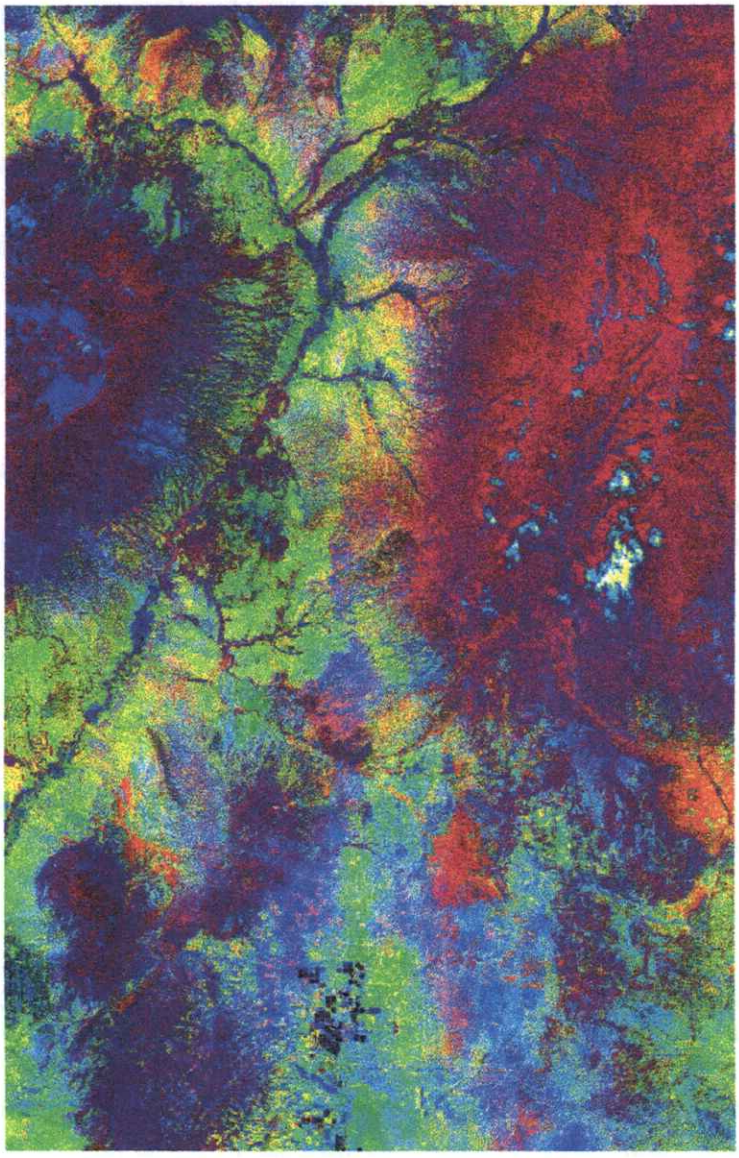

Figure 6. Feature Oriented Principal Component Analysis image. FOPCA-2 in red, FOPCA-1 in green, and FOPCA-3 in blue.

Soil and Vegetation Indices

The images are ordered such that the SMI is in band 1, the NDVI is in band 2, and the SOI is in band 3. As above, the images can be viewed individually to show where the specific surface phenomenon is located or they could be displayed in a 1, 2, and 3 FCC (Figure 7). When displayed together, it will mostly appear as shades of gray indicating that the indices are highly correlated with each other. There are some differences though, such as higher soil moisture in the grasslands of the Estancia Basin as seen in redder hues or higher organic content in the fallow agricultural fields that are blue.

GIS Applications

The above data sets provide a comprehensive set of surface characteristics within the Santa Fe region. The FOPCAs, band ratio images, soil indices, and NDVI provide a range of intensity images for each of the surface features they represent. If these data are calibrated to actual field values, they would be a powerful tool to use in various surface characterization applications that include hydrologic modeling. These images represent a moment in time and may not be an accurate measure of changes over a year or even a season. Therefore, some models may be inappropriate using these single date images. Acquisition and processing of additional dates using satellite imagery would solve this problem. The detailed vegetation/land use classification used in this study is highly adaptive. Depending upon the results desired, re-groupings can be made to illustrate various surface characteristics. A few ideas on how these data sets could be used are described below.

Different types of information can be derived using the vegetation classification in a regrouping procedure. Areas of high human water usage (Classes 30, 31, and 32) combined with areas of high natural water usage (Classes 26, 27, 28, and 29) and surface water (Class 36) would indicate areas where the AET exceeds the potential evapotranspiration. Human and natural barren areas (Classes 33, 34, and 35) indicate areas prone to erosion or high water run-off. Soils with potentially high salt concentrations are indicated by Classes 29 and 17. Over-grazing is indicated by Classes 22, 23, and 25 and in some areas by Classes 16 and 14.

Figure 7. Soil and vegetation indices. SOI in red, NDVI in green, and SMI in blue.

The classification could be combined with other data to create new information. In one study, Blanco-Montero *et al.* (1995) used a Landsat classification over Albuquerque to calculate the amount of AET, insecticide and fertilizer use, yard water use, and total weight of grass clippings generated over a year. In another study, D'Agnese *et al.*(1996) assigned potential evapotranspiration rates to a vegetation classification over Death Valley, Nevada and then used this information with maps of slope, aspect, elevation, and relative rock/soil permeability to create a groundwater recharge map. A simple example of doing this, with products created for this project, is regrouping the classes according to their average values from the soil and vegetation indices (Table 5). This would allow the ability to evaluate the classes as to their relative moisture content (Figure 8) and biomass/AET (Figure 9).

Table 5. Associated index values for each vegetation class.

Class	SMI	NDVI	SOI
1	190.0497	79.0117	204.6396
2	176.3477	103.5332	212.7488
3	176.7196	104.1675	213.5661
4	179.2615	107.0993	214.2319
5	182.7056	107.4377	214.0385
6	186.6706	108.3374	214.4649
7	181.8609	108.4923	213.5791
8	188.5916	109.5665	213.9654
9	189.8013	109.7301	213.456
10	188.1274	110.1286	215.42
11	183.6796	110.5122	213.7025
12	187.5112	110.5771	213.836
13	191.1149	111.1099	213.9563
14	178.0617	112.4209	213.9191
15	179.2279	113.3961	214.4895
16	189.2213	113.4793	214.9618
17	188.2919	113.5205	214.687
18	193.6199	113.7396	215.1051
19	149.2156	114.1071	209.707
20	195.7874	118.3673	214.6167
21	196.334	118.4869	216.0279
22	199.1734	125.3029	214.983
23	194.2101	127.0324	217.949
24	194.8819	128.3393	217.7667
25	201.7199	128.4496	216.7233
26	191.4467	133.0567	222.7093
27	194.833	133.2734	220.629
28	203.7769	138.0485	216.7646

Class	SMI	NDVI	SOI
29	203.4001	142.0199	219.154
30	200.3815	142.9915	225.2995
31	208.8091	144.4211	224.7945
32	206.6139	146.583	223.2484
33	211.5427	146.5864	216.2536
34	207.5342	147.153	217.6168
35	207.1164	148.0748	221.6707
36	209.8439	152.142	219.7836
37	211.8154	156.0136	222.8224

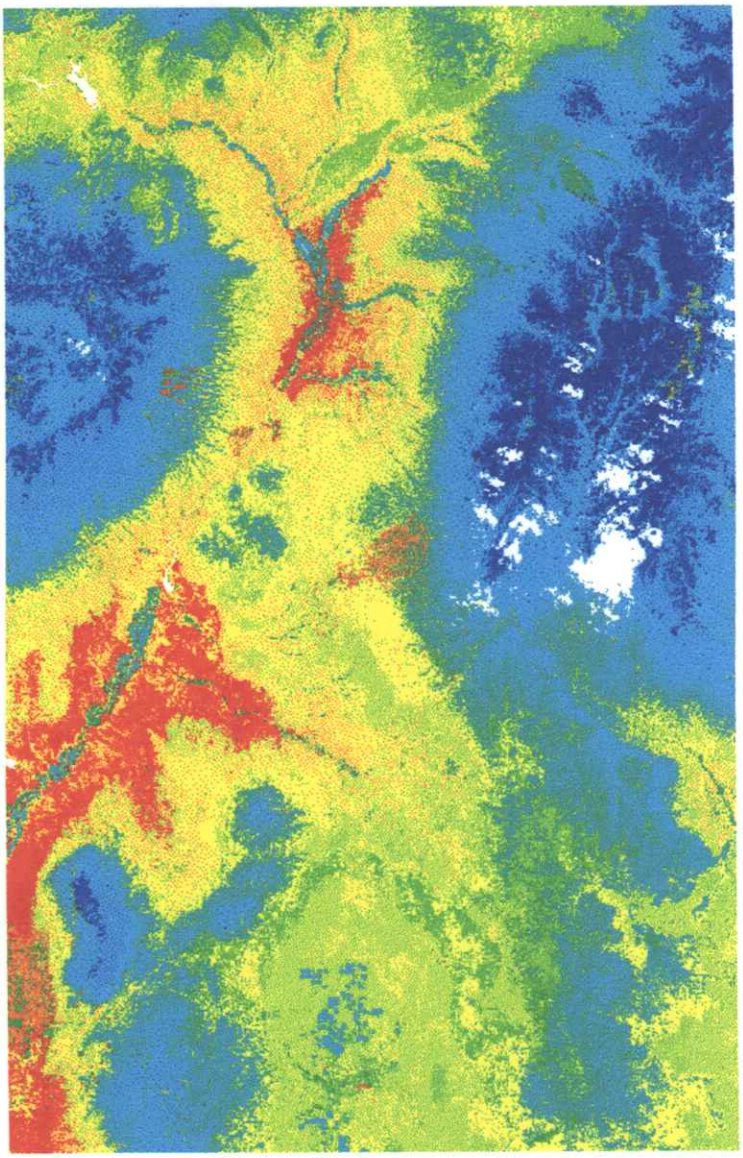

Figure 8. Soil moisture index for each vegetation class. Classes are color coded with the most xeric class in red to the most mesic classes in blue.

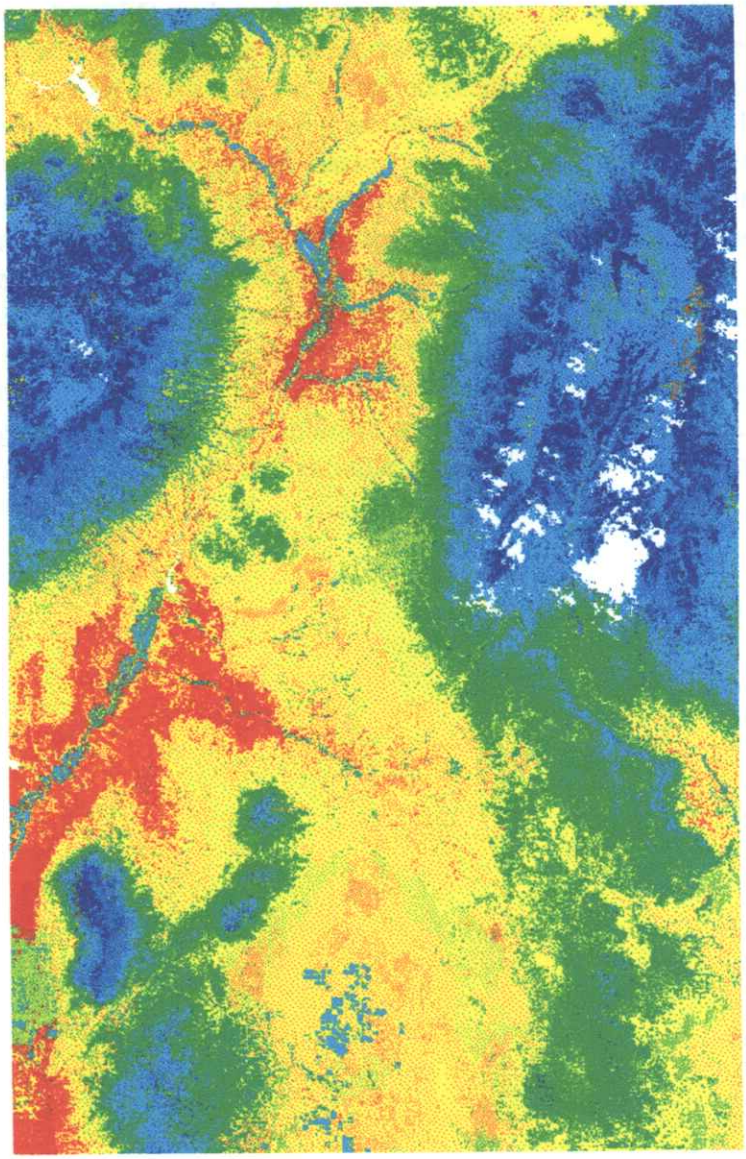

Figure 9. Vegetation index for each vegetation class. Classes are color coded with the least biomass in red to the most biomass in blue.

This could be extrapolated by using the above information with a Digital Elevation Model (DEM) such as described and illustrated below. The reason for doing this is to see where moisture use exceeds natural meteoritic input. The DEM is used as the predictor variable because of the strong correlation between the amount of precipitation and elevation. Using regression analysis, the average SMI and NDVI values from non-disturbance, non-riparian classes were compared to their corresponding DEM values. These classes were used because they represent cover types that are surviving using only meteoritic moisture and therefore would be a reliable indication of the actual moisture regime. Equations predicting SMI and NDVI responses with R^2 greater than 0.85 were derived and applied to the DEM to create separate predicted SMI and NDVI images. These images were then subtracted from the actual SMI and NDVI with the differences highlighting areas of higher than expected soil moisture (Figure 10) and biomass (Figure 11). This would indicate where water demand far exceeds supply. This model is simple and uses only one variable. It could be improved with more research and field calibration.

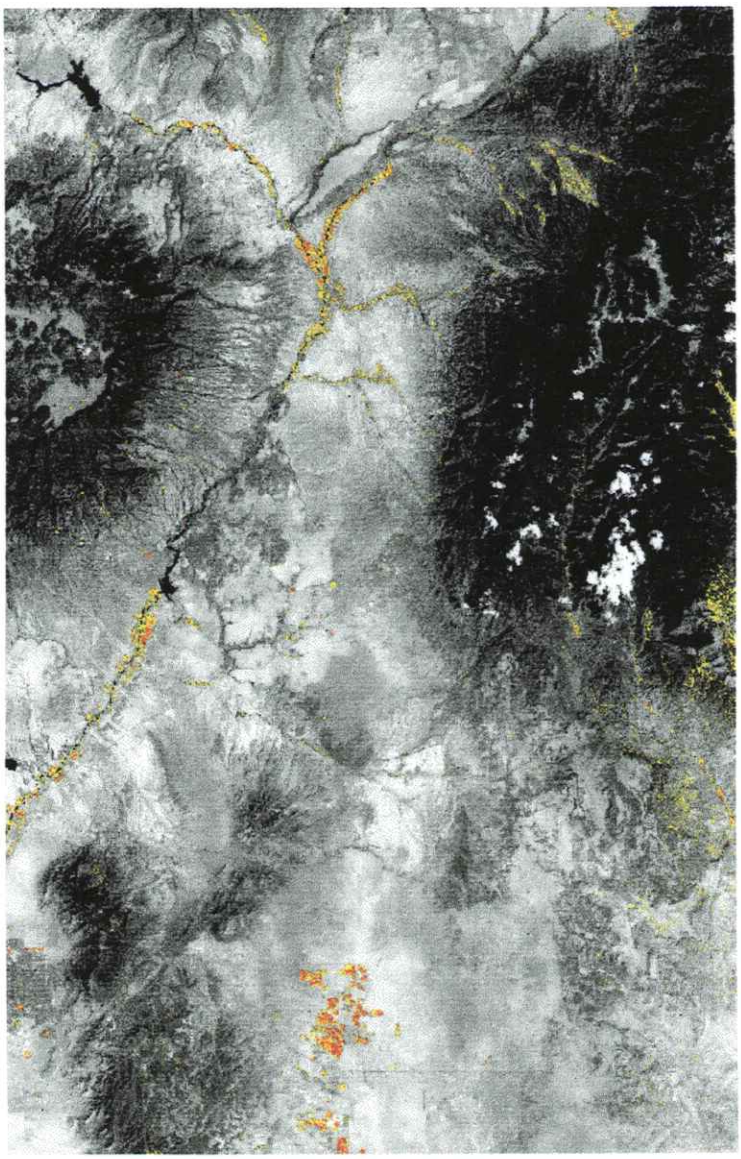

Figure 10. Difference between actual and predicted soil moisture. Yellow to red colors indicate where actual moisture exceeds predicted moisture.

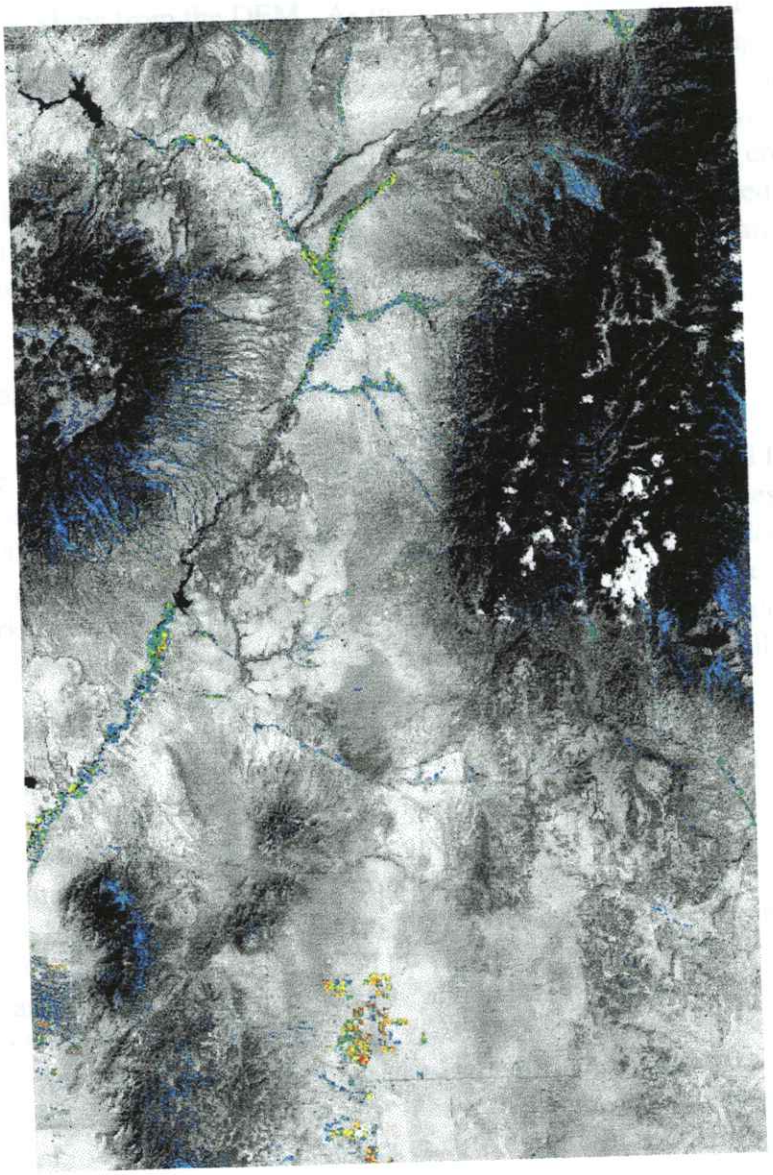

Figure 11. Difference between actual and predicted biomass. Yellow to red colors indicate where actual biomass exceeds predicted biomass.

In another example, a simple erodibility index was created using the inverse of the NDVI and the slope from the DEM. As in the previous example, actual erosion processes are more complicated, but this index can provide a basic understanding of where erosion is occurring and where a potential problem exists. The actual erosion index is shown in Figure 12, with the highest erosion values highlighted in red. In Figure 13, the sub-watersheds are color coded by their sensitivity to erosion. This index could be improved if combined with soil erodibility data from a soil map. This index, used in conjunction with stream net data, could also be used to create a new index that characterizes sensitivity to flooding.

Future Areas of Study

The last sections give some ideas on how this data can be used for multiple applications that include predictive models. The classification provides a 1992 baseline at 1:100,000 scale and the DEM that was used for the elevation and slope information at 1:100,000 scale. The level of use is thereby constrained by these scale parameters. Future work at a watershed or sub-watershed level will require information at a finer scale and, in the case of imagery, will need to be more recent, especially given the rate of change that the Santa Fe region is experiencing.

The enhancements provide a synoptic overview of surface features in 1992. This is fine for general planning purposes, but in order to satisfy specific use, the relationships between the images and surface phenomena will need to be validated and quantified. In particular, equations tying the NDVI response to AET and the SMI to the actual soil moisture can be extremely important to know. These equations may not be universal and may have to change on a basin by basin procedure. Elevation was the only variable used to model naturally-occurring soil moisture and biomass profiles. The picture is more complicated and therefore justifies other variables such as soil texture or aspect to be included to more accurately model these surface characteristics. Likewise, the erodibility index provided a simple demonstration on how to use this information for an application, but would improve with additional research into the use of soil data, connectivity analysis and predicted runoff,as well as other variables.

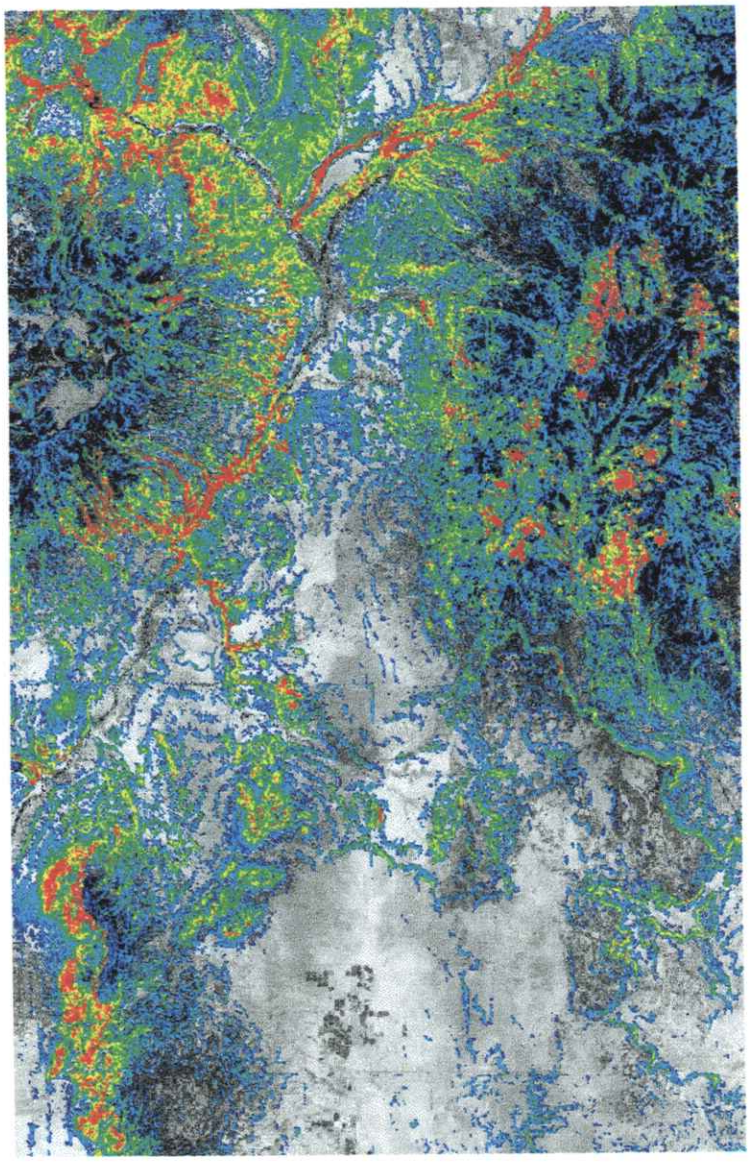

Figure 12. Erosion index. Blue to red colors indicate increasing sensitivity to erosion.

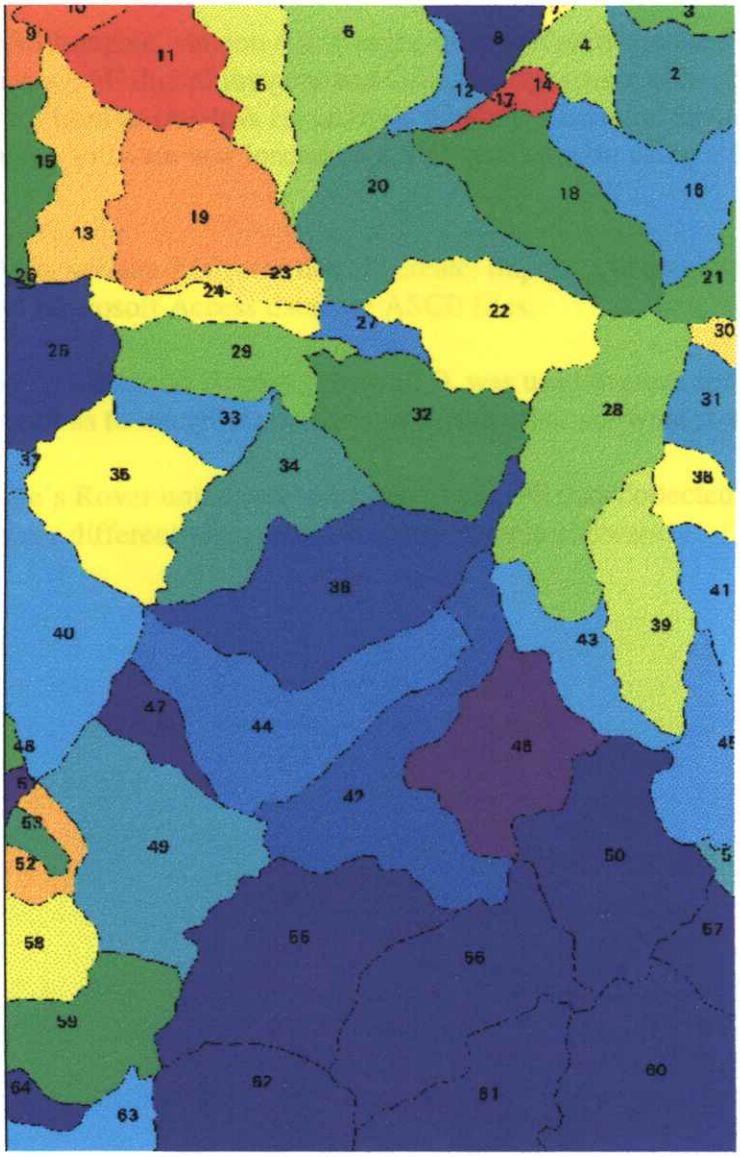

Figure 13. Sub-watersheds color-coded by erosion index. Blue to red colors show increasing sensitivity to erosion.

Software and Hardware Used

ERDAS Imagine, version 8.x, was the principal software used throughout the mapping process. All digital imagery and GIS coverages were either processed, manipulated, or used as overlays for analysis within the Imagine environment. The ERDAS Imagine software was loaded on a SUN workstation using a SUN OS Unix operating system.

Arc/Info, version 7.03, was used to create, import, and manipulate vector coverages and Microsoft Access database ASCII files.

PC based Microsoft Access, version 2.0, was used to store and manipulate all field data as well as to integrate ancillary data from other software sources.

Trimble's Rover units were used to collect GPS data collected in the field. All coordinates were differentially corrected using Trimble software.

References

Bastiaanssen, W.G.M., T. Van Der Wal, and T.N.M. Visser, 1996. Diagnosis of Regional Evaporation by Remote Sensing to Support Irrigation Performance Assessment. *Irrigation and Drainage Systems*, 10:1-23.

Blanco-Montero, C.A., T.B. Bennett, P. Neville, C.S. Crawford, B.T. Milne, and C.R. Ward, 1995. Potential Environmental and Economic Impacts of Turfgrass in Albuquerque, New Mexico. *Landscape Ecology*. 10:121-128.

Carlson, T.N, W.J. Capehart, and R.R. Gillies, 1995. A New Look at the Simplified Method for Remote Sensing of Daily Evapotranspiration. *Remote Sensing of the Environment*, 54:161-167.

Choudhury, B.J., N.U. Ahmed, S.B. Idso, R.J. Reginato, and C.S.T. Daughtry, 1994. Relations Between Evaporation Coefficients and Vegetation Indices Studied by Model Simulations. *Remote Sensing of the Environment*, 50:1-17.

Coleman, T.L., and O.L. Montgomery, 1987. Soil Moisture, Organic Matter, and Iron Content Effect on the Spectral Characteristics of Selected Vertisols and Alfisols in Alabama. *Photogrammetric Engineering and Remote Sensing*. 53:1659-1663.

Crosta, A.P., and J. McM. Moore, 1989. Enhancement of Landsat Thematic Mapper Imagery for Residual Soil Mapping in SW Minas Gerais State, Brazil: A Prospecting Case History in Greenstone Belt Terrain. *Seventh Thematic Conference on Remote Sensing for Exploration Geology, Calgary, Canada*:1173-1187.

Culler, R.C., R.L. Hanson, and J.E. Jones, 1976. Relation of the Consumptive Use Coefficient to the Description of Vegetation. *Water Resources Research*, 12:40-46.

D'Agnese, F.A., C.C. Faunt, and A.K. Turner, 1996. Using Remote Sensing and GIS Techniques to Estimate Discharge and Recharge Fluxes for the Death Valley Regional Groundwater Flow System, USA. *HydroGIS 96: Application of Geographic Information Systems in Hydrology and Water Resources Management* (Proceedings of the Vienna Conference). IAHS Publication 235:503-511.

Dick-Peddie, W.A., 1993. *New Mexico Vegetation – Past, Present and Future.* University of New Mexico Press:Albuquerque, NM, 244pp.

ERDAS, 1997. *ERDAS Field Guide*. ERDAS, Inc: Atlanta, GA, 656 pp.

Lillesand, T.M., and R.W. Kiefer, 1987. *Remote Sensing and Image Interpretation (2nd Edition).* John Wiley & Sons, Inc.:Toronto, Canada, 721 pp.

Morris, W.S., and K.W. Haggard, 1985. New Mexico Climate Manual: Solar and Weather Data. *New Mexico Energy Research and Development Institute* 2-72-4523, 601 pp.

Sabins, F.F. Jr., 1987. *Remote Sensing – Principles and Interpretation (2nd Edition).* W.H. Freeman and Company: New York, NY, 449 pp.

Appendix A

Santa Fe County Region

Map Units Descriptions

(Descriptions are based in part on Dick-Peddie [1993]. Although the indices have not been field validated they are ranked for each class in the description to give a general picture as to how the classes relate to each other and to the features described by the indices. Index rankings go from lowest to highest ranks, 1-35, representing lowest to highest values)

Map Unit No. 1 (Acres: 7,242)

Alpine Tundra Vegetation

This covers the highest peaks in the region (above 11,500 feet). Vegetation can include willow species (*Salix spp.*), sedges, rushes and avens. The harsh environment for this class means relative undeveloped soils (lowest SOI) and high erosion sensitivity despite having some of the highest precipitation as indicated by the high SMI and NDVI.

SMI – 32 NDVI – 29 SOI – 1 EI - 34

Map Unit No. 2 (Acres: 10,158)

Alpine Tundra Rock Field

This unit covers the highest peaks in the region (above 11,500 feet). It is mainly made up of talus slopes and other barren areas. Besides lichens other vegetation may include dwarf, wind-shappen shrubs "krummholz" type communities with plants such as bristlecone pine (*Pinus aristata*). Although similar in its environment to Class 1, its increase harshness is indicated by a lower SMI and NDVI, and the highest EI. The higher SOI may be due to a geologic response rather than actually having a better developed soil than Class 1.

SMI – 26 NDVI – 23 SOI – 3 EI - 35

Map Unit No. 3 (Acres: 48,757)

Subalpine Broadleaf Forest (Aspen)

This is the highest elevation broadleaf forests and is dominated by aspen (*Populus tremuloides*). Most of these forests are signs of past disturbance where fire, landslides, disease, or logging has taken out the conifers that were there previously. This has the highest SMI and NDVI of all the classes reflecting the high biomass in the area with the highest precipitation. Surprisingly, the SOI is very low which may be due to the disturbance nature of the class; whatever soil development occurred under the previous conifer community may have been washed out with the destruction of the forest and now the soil just beginning to develop again.

SMI – 35 NDVI – 35 SOI – 5 EI - 20

Map Unit No. 4 (Acres: 100,120)

Subalpine Conifer Forest (Englemann Spruce)

This is the highest elevation conifer forest and is dominated by Englemann spruce (*Picea englemannii*). Other conifers may be locally dominant such as pine species (*Pinus flexilis* and *P. aristata*) and subalpine fir (*Abies lasiocarpa*). This has one of the highest SMI and NDVI rankings, but being a conifer community the soils are relatively poor. The high slopes and poor soils make this area a high EI.

SMI – 34 NDVI – 31 SOI – 13 EI - 28

Map Unit No. 5 (Acres: 168,160)

Subalpine Conifer Forest (Englemann Spruce, Subalpine Fir, and Aspen)

High elevation conifer forest which is dominated by Englemann spruce (*Picea englemannii*), subalpine fir (*Abies lasiocarpa*), and aspen (*Populus tremuloides*). This class is in a similar environment to Class 4, although the addition of the Aspen to this community creates a higher NDVI response.

SMI – 33 NDVI – 34 SOI – 12 EI - 25

Map Unit No. 6 (Acres: 266,897)

Upper Montane Conifer Forest (Douglas-fir, White Fir, and Blue Spruce)

These mid-elevation conifer forests are dominated by Douglas-fir (*Pseudotsuga menzeisii*), white fir (*Abies concolor*), and blue spruce (*Picea pungens*). Lower elevations will also have Ponderosa Pine (*Pinus ponderosa*) and Gambel *oak (Quercus gambelii*). These forests are a little more xeric than the previous forest classes, but tend to be on higher slopes and therefore have a higher EI.

SMI – 31 NDVI – 32 SOI – 14 EI - 30

Map Unit No. 7 (Acres: 385,198)

Lower Montane Conifer Forest (Ponderosa Pine)

The lowest elevation conifer forest, this forest is dominated by Ponderosa *Pine (Pinus ponderosa*). It can occur as grassy savannas or with pinyon (*Pinus edulis*), juniper species (*Juniperus monosperma* and *J. scopulorum*), or Gambel oak (*Quercus gambelii*) as sub-canopies. The most xeric of the conifer forest, nutrients are very limited and the soil is poor which is reflected in the low SOI.

SMI – 28 NDVI – 26 SOI – 6 EI - 27

Map Unit No. 8 (Acres: 58,186)

Montane Deciduous Scrub (Gambel Oak, Mountain Mahogany, and New Mexico Locust)

Mid-elevation scrub dominated by Gambel oak (*Quercus gambelii*), mountain mahogany (*Cercocarpus montanus*), and New Mexico locust (*Robinia neomexicana*).

SMI – 30 NDVI – 33 SOI – 11 EI - 18

Map Unit No. 9 (Acres: 43,298)

Evergreen Interior Chaparral (Scrub Oak, Wavyleaf Oak, and Mountain Mahogany)

This is a more xeric scrub community dominated by oak species (*Quercus turbinella* and *Q. undulata*) and mountain mahogany (*Cercocarpus montanus*). This scrub tends to be found on dry, rocky slopes.

SMI – 14 NDVI – 15 SOI – 4 EI - 22

Map Unit No. 10 (Acres: 368,691)

Closed Conifer Woodland (Pinyon with Juniper and Oak species)

Pinyon (*Pinus edulis*) and juniper species (*Juniperus monosperma and J. scopulorum*) dominated closed woodland with oak species (*Quercus undulata and Q. gambelii*). Big sagebrush (*Artemisia tridentata*) and mountain mahogany (*Cercocarpus montanus*) can be locally dominant. The most mesic of the closed conifer woodlands.

SMI – 24 NDVI – 20 SOI – 21 EI - 23

Map Unit No. 11 (Acres: 335,982)

Closed Conifer Woodland (Pinyon and One-Seed Juniper with Grama grasses)

Pinyon (*Pinus edulis*) and one-seed (*Juniperus monosperma*) dominated closed woodland with grama grasses (*Bouteloua gracilis* and *B. curtipendula*). Other grass species are locally dominant such as the muhly species (*Muhlenbergia spp.*), needlegrass species (*Stipa spp.*), galleta (*Hilaria jamesii*), and Indian ricegrass (*Oryzopsis hymenoides*).

SMI – 22 NDVI – 18 SOI – 7 EI - 17

Map Unit No. 12 (Acres: 83,326)

Closed Conifer Woodland (Pinyon and One-Seed Juniper with sparse ground cover)

Pinyon (*Pinus edulis*) and one-seed juniper (Juniperus monosperma) dominated closed woodland on sparsely covered soils. These woodlands tend to be found on highly dissected, sloping terrain. These woodlands tend to have poor soils and be on high slopes and is therefore one of the most sensitive to erosion.

SMI – 12 NDVI – 16 SOI – 8 EI - 33

Map Unit No. 13 **(Acres: 24,003)**

Open Conifer Woodland (One-Seed Juniper with Oak species)

One-seed juniper (*Juniperus monosperma*) dominated open woodland with oak species (*Quercus undulata and Q. turbinella*). Big sagebrush (*Artemisia tridentata*) and mountain mahogany (*Cercocarpus montanus*) can be locally dominant. The most mseic of the open woodlands.

SMI – 23 NDVI – 19 SOI – 10 EI - 9

Map Unit No. 14 **(Acres: 634,683)**

Open Conifer Woodland (One-Seed Juniper with Grama grasses)

One-seed (*Juniperus monosperma*) dominated open woodland "savanna" with grama grasses (*Bouteloua gracilis, B. eriopoda,* and *B. curtipendula*). Other grass species are locally dominant such as the muhly species (*Muhlenbergia spp.*), needlegrass species (*Stipa spp.*), galleta (*Hilaria jamesii*), and Indian ricegrass (*Oryzopsis hymenoides*).

SMI – 10 NDVI – 11 SOI – 9 EI - 24

Map Unit No. 15 (Acres: 249,780)

Open Conifer Woodland (One-Seed Juniper with sparse cover)

One-seed juniper (Juniperus monosperma) dominated open woodland "savanna" on sparsely covered soils. This woodland tends to be found on poor soils and highly dissected, sloping terrain and is therefore sensitive to erosion.

SMI – 6 NDVI – 6 SOI – 15 EI - 31

Map Unit No. 16 (Acres: 184,642)

Microphyllous Desert Shrubland (Bigleaf and Sand Sagebrush with Rabbitbrush and Fourwing Saltbush)

Desert shrubland dominated by sagebrush species (*Artemisia tridentata* and *A. frigida*) as well as other shrubs such as rabbitbrush species (Chrysothamnus spp.) and fourwing saltbush (Atriplex canescens). Soils tend to be sandy and in some places can be dunal.

SMI – 15 NDVI – 8 SOI – 18 EI - 19

Map Unit No. 17 (Acres: 9,694)

Microphyllous Desert Shrubland (Fourwing Saltbush with Greasewood)

Desert shrubland dominated by fourwing saltbush (*Atriplex canescens*) and in some areas by greasewood (*Sarcobatus vermiulatus*). Ground cover is sparse although locally dominant in forbs and sacaton grasses (*Sporobolus airoides* and *S. giganteus*). Soils tend to be clay-rich and saline.

SMI – 7 NDVI – 4 SOI – 17 EI - 26

Map Unit No. 18 (Acres: 64.202)

Subalpine/Montane Grassland (Fescue species)

High altitude grassy meadows and montane valleys which include fescue species (Festuca spp.), other cool, mesic (C3) grass species. Sedge and rush wetlands can also be locally dominant. The most mesic of the grasslands and some of the best soil development in the mountains except in the riparian areas.

SMI – 29 NDVI – 30 SOI – 20 EI - 15

Map Unit No. 19 (Acres: 16,830)

Mid-Grass Prairie (Needlegrass species with other grass species)

Mid-grass prairie dominated by Needlegrass species (*Stipa comata* and *S. neomexicana*) as well as other mid-grass species and shrubs. This grassland tends to be found on shallow, carbonate, sandy, or rocky soils.

SMI – 18 NDVI - 17 SOI - 2 EI - 7

Map Unit No. 20 (Acres: 34,791)

Mid-Grass Prairie (Side-Oats Grama mixed with Beargrass and other grass species)

Grasslands dominated by sideoats grama (*Bouteloua curtipendula*) found mainly on the lower slopes of mountains or foothills. Beargrass (*Nolina microcarpa*) as well as other grass species are also found in this class. Soils tend to be shallow, rocky and highly sloping and therefore is sensitive to erosion.

SMI – 8 NDVI – 10 SOI – 16 EI - 29

Map Unit No. 21 **(Acres: 497,057)**

Short-Grass Prairie (Blue Grama mixed with other grass species)

Short-grass prairie and Great Basin grassland which is dominated by blue grama (*Bouteloua gracilis*). Other grasses such as galleta (*Hilaria jamesii*), western wheatgrass (*Agropyron smithii*) and Indian ricegrass (*Oryzopsis hymenoides*, as well as shrubs and forbs are locally dominant. Though it has a low biomass response compared to the other classes, the build up of sod gives it a reltively high SOI.

SMI – 13 NDVI – 7 SOI – 22 EI - 10

Map Unit No. 22 **(Acres: 70,331)**

Short-Grass Prairie (Blue Grama mixed with Cholla, Sagebrush, Juniper and other grass species)

Short-grass prairie and Great Basin grassland which was originally dominated by blue grama (*Bouteloua gracilis*), but is now a highly disrupted system, most likely by excessive grazing pressures or other human development. There are large concentrations of cholla (*Opuntia imbricata*), sagebrush species (*Artemisia tridentata, A. frigida, A. ludoviciana*), one-seed juniper (*Juniperus monosperma*), snakeweed species (*Gutierrezia spp.*), other grasses such as galleta (*Hilaria jamesii*), western wheatgrass (*Agropyron smithii*) and Indian ricegrass (*Oryzopsis hymenoides*, and mixed forbs. These grasslands may turn into open conifer woodlands if the disturbance pressures are not mitigated.

SMI – 16 NDVI – 12 SOI – 19 EI - 8

Map Unit No. 23 (Acres: 111,326)

Short-Grass Prairie (Blue Grama mixed with Snakeweed and other grass species)

Short-grass prairie and Great Basin grassland which was originally dominated by blue grama (*Bouteloua gracilis*), but is now a highly disrupted system, most likely by excessive grazing pressures, and therefore has large concentrations of snakeweed species (*Gutierrezia spp.*), other grasses such as galleta (*Hilaria jamesii*), western wheatgrass (*Agropyron smithii*) and Indian ricegrass (*Oryzopsis hymenoides*, and mixed forbs. In many *areas G. spp.* is actually the dominant plant species. A very high SOI either may be due to a lithologic response or may indicate that the *G. spp.* may provide more organic material.

SMI – 9 NDVI – 5 SOI – 28 EI - 12

Map Unit No. 24 (Acres: 35,753)

Desert Grassland (Black Grama mixed with other grass species)

Desert grassland dominated by black grama (*Bouteloua eriopda*) although other grass species, shrubs and forbs can be locally dominant. As is seen by the SMI and the NDVI, this is the most xeric class, but it has a remarkably high SOI which may be due to organic build up or may be due to a lithologic/soil response.

SMI – 1 NDVI – 1 SOI – 27 EI - 21

Map Unit No. 25 **(Acres: 127,249)**

Desert Grassland (Black Grama mixed with Snakeweed and other grass species)

Desert grassland which was originally dominated by black grama (*Bouteloua eriopda*), but it is now a highly disrupted system, most likely by excessive grazing pressure, and therefore has large concentrations of snakeweed species (*Gutierrezia spp.*), disturbance grasses such as aristida species (*Aristida spp.*), and mixed forbs. In many *areas G. spp.* is actually the dominant plant species. This class also shows the same inverse relationship between soil moisture and active biomass as compared to organics in the soil.

SMI – 2 NDVI – 2 SOI – 24 EI - 16

Map Unit No. 26 **(Acres: 5,898)**

Montane Riparian (Willow species, Sedges and Rushes)

High elevation stream-side communities with a high diversity of species. Willow species are found throughout and sedges and rushes are found in open wetlands. Other common species include Cottonwood species (*Populus angustifolia* and *P. deltoides*), boxelder (*Acer negundo*), gambel oak (*Quercus gambelii*), and netleaf hackberry (*Celtis reticulata*). This community shows some of the highest soil moisture, biomass response, and soil development.

SMI - 27 NDVI - 27 SOI - 32 EI - 13

Map Unit No. 27 **(Acres: 25,674)**

Riverine Bosque (Cottonwood, Russian Olive, Tamarisk, and Willow species)

Lower elevation floodplains with tall, enclosed "gallery" forests dominated by Cottonwood *(Populus deltoidies*), but can have significant cover of Russian Olive (*Elaeagnus angustifolia*), Tamarisk (*Tamarix spp.*), and Willow species (*Salix goodingii* and *S. exigua*). This has high organic content in the soils and has a much higher soil moisture and biomass response compared to the woodland, shrubland and grassland communities it passes through.

SMI - 21 **NDVI -** 22 SOI - 30 **EI** – 4

Map Unit No. 28 (Acres: 3,486)

Riverine Woodland (Tamarisk, Russian Olive, and Willow species)

Lower elevation floodplains with a smaller closed woodland dominated by Tamarisk (*Tamarix spp.*), as well as Russian Olive (*Elaeagnus angustifolia*), and Willow species (*Salix goodingii and S. exigua*). These areas were probably once dominated by Cottonwood (*Populus deltoidies*), *S. Goodingii* and *S. exigua*. This tends to be located in more xeric drainages than Class 27.

SMI - 19 NDVI - 21 SOI - 25 EI – 2

Map Unit No. 29 (Acres: 3,451)

Arroyo Shrubland (Tamarisk, Fourwing Saltbush, and Greasewood)

Drainages dominated by tamarisk (*Tamarix spp.*), fourwing saltbush (*Atriplex canescens*), and greasewood (*Sarcobatus vermiculatus*). Ground cover is sparse although locally dominant in forbs and sacaton grasses (*Sporobolus airoides* and *S. giganteus*). These drainages tend to be ephemeral, clay-rich and highly saline.

SMI - 11 NDVI - 9 SOI - 29 EI - 3

Map Unit No. 30 (Acres: 38,151)

Irrigated Agriculture

Areas of irrigated agriculture. The indices are what is expected for an area that receives large amounts of irrigation, undergoes much soil preparation (highest SOI), and are levelled (lowest EI).

SMI - 25 NDVI - 28 SOI - 35 EI - 1

Map Unit No. 31

(Acres: 4,835)

Parks, Golf Courses, and Irrigated Pastures

Areas of irrigated turfgrass such as parks or golf courses or irrigated pastures of alfalfa or feed. Similar to Class 30, but more xeric.

SMI - 17 NDVI - 24 SMI - 34 EI - 5

Map Unit No. 32

(Acres: 14,542)

Mesic Rural/Residential (Mixed trees and irrigated grasses)

Mixed trees and lawns or other mesic human development.

SMI - 20 NDVI - 25 SMI - 33 EI - 6

Map Unit No. 33

(Acres: 18,815)

Xeric Residential/Urban (Barren or sparsely vegetated)

Areas including barren lots, roads, and xeric landscaping.

SMI - 4 NDVI - 14 SOI - 23 EI - 11

Map Unit No. 34

(Acres: 19,681)

Manmade Barren (Roads, dams, and etc...)

Manmade barren areas including asphalt and concrete roads, dams, parking lots, large shopping centers and industrial areas. Higher than expected NDVI may be due to disturbance forbs and weeds which will remain green long after other vegetation has gone dormant.

SMI - 3 NDVI - 13 SOI - 26 EI - 14

Map Unit No. 35 (Acres: 60,808)

Rock Outcrop/Talus/Barren or Sparsely Vegetated

Areas of sparse to no vegetation including rock outcrops, talus slopes, and barren flats. It has a high erosion index, although this includes a mix of slopes and rock/soil types. The high SOI may be due a lithologic response.

SMI - 5 NDVI - 3 SOI - 31 EI - 32

Map Unit No. 36 (Acres: 6,457)

Surface Water

Lakes, rivers, and other standing bodies of water.

Map Unit No. 37 (Acres: 53,483)

Clouds and Shadows

Areas where clouds and shadow cover the image.